

# A new rotor balancing method based on PTFA theory<sup>1</sup>

JIANG HONG<sup>2</sup>, SHI YONGFANG<sup>3,4</sup>, RAN XIANGFENG<sup>2</sup>

**Abstract.** Whether the large rotating machinery can run smoothly is closed related to the dynamic balance quality of the rotor, and the dynamic balance technology plays a very important role in the operation and maintenance of the unit. Aiming at the shortage of the current rotor balancing method for processing non-stationary data, the paper applies PTFA (parameterized time-frequency analysis) and holo-balancing method together to determine the unbalance weight and unbalance angle of the rotor. The method rotates the time-frequency characteristics of the rotor run-up vibration signal to extract the rotating frequency component. By adding the trial weight and obtaining the transfer matrix under various speeds, the method can avoid the shortcoming of the traditional rotor balancing method. Experimental results show that this method can reduce unbalanced vibration of the rotor system at working speed and critical speed.

**Key words.** Balancing method, PTFA, rotor, run-up signal.

## 1. Introduction

Rotor is the core component of rotary machine, whose vibration problem is inevitable. Rotor imbalance is the most common fault of rotary machine. In order to eliminate or reduce the vibration of the rotor system, we should firstly consider the balance of the rotor.

As early as 1919, Jeffcott raised the need for the dynamic balance of the rotor. Dynamic balance mostly involved rigid rotors alone before the 1950s. But in fact, lots of rotors worked at the first-order critical speed or above the second-order critical speed as their working speed and load continued to increase. The actual needs then promoted the research on methods for the dynamic balance of the flexible rotor. In the past few decades, a series of dynamic balancing methods, techniques and equipment for flexible rotors have been developed at home and abroad. Grobel,

---

<sup>1</sup>This study is supported by the Science and Technology Supporting of Xinjiang Uygur Autonomous Region(Grant No. 2015211C256)

<sup>2</sup>School of Mechanical Engineering, Xinjiang University, Urumqi, Xinjiang, 8300046, China

<sup>3</sup>School of Medical Engineering, Xinjiang Medical University, 830011,China

<sup>4</sup>Corresponding author

Bishop, Federn and his collaborators laid the foundation for the vibration balancing method, later known as modal balancing [1]. When the modal balancing approach arose in Western Europe, the influence coefficient method [2] came into being in the United States. In 1963, Goodman proposed the use of least squares in the influence coefficient method as its biggest advantage lies in electronic computer-aided dynamic balance which helps to establish a practical multi-plane multi-speed influence coefficient balancing method. In order to further improve this method, a large number of theoretical studies and experiments have been conducted and then many improvement measures have been put forward, contributing to the wide application of the influence coefficient method in practice. Despite constant improvement and development, the above two flexible rotor balancing methods still have their own insurmountable problems.

Based on linear vibration theory, the influence coefficient method works out the calibration quality using the linear relationship between unbalance vector and vibration vector. Modal balancing method relies on the orthogonal principle of rotor vibration mode to keep balance. The vibration of each order rotor vibration mode can only be caused by the corresponding imbalance of vibration mode. If to reduce the vibration of the rotor system, we shall revise the imbalances of each order vibration mode respectively.

Regardless of influence coefficient method or modal balancing method, both of them are based on rotor steady-state response, that is, with the steady-state response data of rotor system under some selected speed, the calibration quality is determined by the steady-state response before and after the trial weight at a balanced speed [3]. Under field balance, we need to carry out many trials to determine the calibration quality. However, the balancing efficiency is low, in addition, we can not ensure the small vibration at other speeds. If the rotor balancing can be rapidly achieved by the transient response data through rotor startup process, it is significantly important to reduce the rotor vibration at all speeds [4].

The rotor startup signals contain rotating frequency component, doubling frequency component and sub-doubling frequency components. Moreover, the vibration of rotating frequency component is mainly related to rotor imbalance. Therefore, it is extremely important for the subsequent rotor balancing to accurately extract the amplitude phase of rotational frequency component during the rotor startup process.

The rotor startup signals are the typical non-stationary signals. In order to effectively study these non-stationary signals, time-frequency analysis has received widespread concern. The basic idea is to construct the joint function of time and frequency through mapping the one-dimensional time domain signal into two-dimensional time-frequency plane. Furthermore, it is also used to describe the energy density and intensity of the signals at different time and frequency [5].

The common time-frequency analysis methods mainly include Short-time Fourier Transform (STFT), Wavelet Transform, Wigner-Ville Distribution and Empirical Mode Decomposition (EMD). When analyzing non-stationary signals, these methods have the following limitations:

- 1) The time-frequency resolution ratio of STFT is only related to window function. The size and shape of window-field can not be changed with that of the signal

frequency, which lacks self-adaptability.

2) Under the restriction of uncertainty principle, Wavelet Transform can not achieve a high resolution both in time and frequency domains. Once selected, the wavelet can not change throughout the signal analysis process.

3) Wigner-Ville Distribution will be seriously interfered by the cross term when analyzing multi-component signals.

4) EMD has the issues like end effect, mode mixing and so on.

All the time-frequency analysis methods mentioned above have no a priori assumed signal models, and assume the signals to be analyzed as quasi stationary signals to different extent, which is therefore referred to as non-parametric time-frequency method.

Yang Yang and other researchers [6] proposed a new method to analyze non-stationary signal, which is called parameterized time-frequency analysis, whose essential idea is to carry out the time-frequency domain rotation through constructing the transform kernel that matches the signals, so that the concentricity represented by signal time-frequency will be optimal. Based on the parameterized time-frequency analysis, the author decomposes the rotating frequency vibration signals from the startup vibration signals. Combined with the holobalancing method [7], the balance of the rotor under all working conditions is achieved.

## 2. The extract of rotating frequency component during the rotor startup process

### 2.1. The basic theory of parameterized time-frequency analysis

The rotor startup signals are the multi-components signals of frequency modulation and amplitude modulation.

$$z(t) = \sum_{i=1}^N A_i(t) \exp \left\{ j \left[ 2\pi \int f_i(t) dt + \phi_i(t) \right] \right\}. \quad (1)$$

Here,  $A_i(t)$ ,  $f_i(t)$  and  $\phi_i(t)$  are, respectively, the amplitude, frequency and phase of the  $i$ th signal component. The number of signal components is  $N$ . All of them are the functions varying with time, and the frequency variation function of rotating frequency component can be fitted by using the key-phase signals.

In view of the above startup signals, and combined with the frequency variation function of rotating frequency signals, the matching rotating operator can be constructed.

$$\Phi^R(t) = \exp \left\{ -j \left[ 2\pi \int f(t) dt \right] \right\}. \quad (2)$$

In this way we will obtain a rotation field after rotating the original signals in

the form

$$\text{RTF}_S(t, w, P) = \int_{-\infty}^{+\infty} z(\tau)\Phi^R(\tau)h(\tau - t) \exp(-j\omega\tau) d\tau. \quad (3)$$

The above formula represents the parameterized rotary time-frequency transform. The function of the rotating operator is to rotate the time-frequency feature to a fixed frequency in the time-frequency representation, and to make the signals after the time-frequency rotation pass through the band-pass filter, so as to extract the rotating frequency component during the startup process. The specific decomposition steps are as follows:

(a). Firstly, combined with the frequency variation function of rotating frequency signals, the rotating operator is constructed. Fig. 1(a) and Fig. 2(a) are, respectively, the time domain figure and time-frequency spectrum of the original startup signal.

(b). Rotating the original startup signal, Fig.1 (b) and Fig. 2(b) are, respectively, the time domain figure and time-frequency spectrum of the signal after rotating. According to Fig. 2(b), the time-frequency feature of the rotating frequency component after rotating is completely parallel to the time axis, and is always the initial frequency of the component.

(c). Taking as the center frequency, the zero-phase band-pass filter is designed. After filtering the rotating signal, we will get the filtered signal; Fig. 1(c) and Fig. 2(c) are respectively the time domain figure and time-frequency spectrum of filtered signal.

(d). Rotating the filtered signal through the rotating operator.

Thus, extracting the rotating frequency component, Fig. 1(d) and Fig.2 (d) are, respectively, the time domain figure and time-frequency spectrum of the rotating frequency component.

## ***2.2. The drawing of rotating frequency component Bode diagram***

Bode diagram is common method used to analyze the rotor startup information, which can visually display the amplitude and phase of the rotor vibration varying with the speed during the startup process. The traditional drawing method of Bode diagram is discontinuous sampling, which means to collect multiple sets of data during the process of speeding-up. Finally, by connecting all the data points, we will get the Bode diagram, which has a different degree of distortion[8]. This thesis uses the method of achieving the vibration signal complex envelope to draw Bode diagram of the rotor rotating frequency component, which not only reduce the number of signal acquisition, but ensure the accuracy of the Bode diagram.

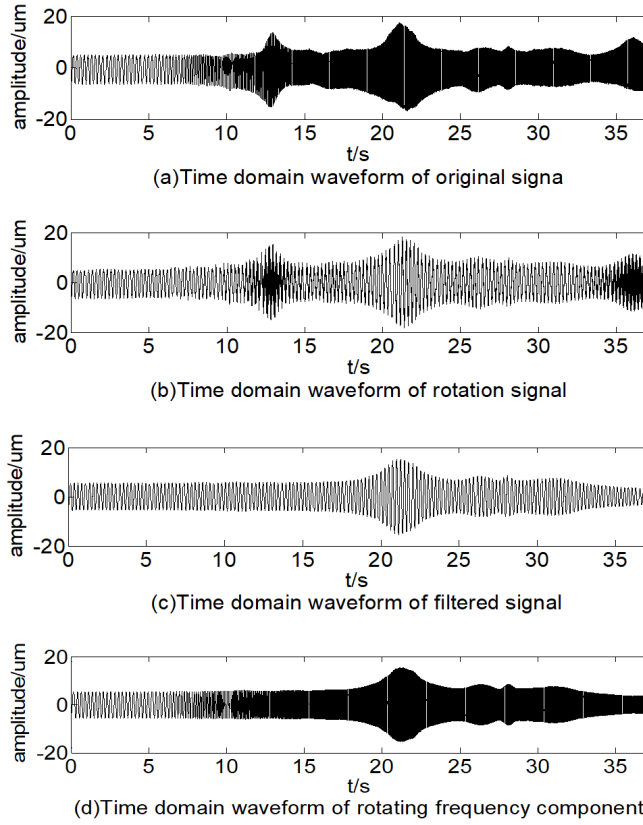


Fig. 1. Time domain waveform of the extraction of rotating frequency component

### 3. Analysis and experimental verification of simulation signals

#### 3.1. Analysis of simulating signals

In order to verify the accuracy of the parameterized time-frequency analysis method extracting the rotating frequency component, the author has carried out the simulation signal analysis and test bench verification respectively. The simulation signals use Jeffcott model.

Although the coincidence of rotating frequency component extracted by parameterized time-frequency analysis and theoretical rotating frequency component can be observed through the waveform directly, we also have to conduct a quantitative evaluation on the accuracy of the extraction results. This paper uses the root mean square error (RMSE) as the evaluation index

$$\text{RMSE} = \sqrt{\frac{\sum_{j=1}^n (s_i - x_i)^2}{n}}. \quad (4)$$

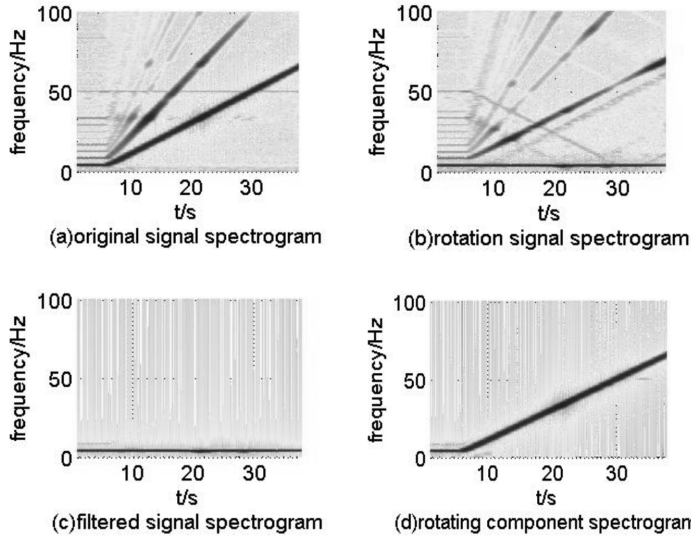


Fig. 2. Time-frequency domain spectrogram of the extraction of rotating frequency component

In formula (4),  $s_j$  is the discrete value of rotating frequency component extracted by parameterized time-frequency analysis  $x_j$  is the discrete value of theoretical rotating frequency component, an  $n$  is the number of discrete points.

After calculating, the root mean square error of rotating frequency component extracted by parameterized time-frequency analysis and theoretical rotating frequency component is 0.0578, which illustrates that the parameterized time-frequency analysis can accurately extract the rotating frequency component.

### 3.2. The experiment of steady-state startup

The methodology is experimentally verified on Bently RK4 rotor test bench. In order to fully consider the effects of all rotors supporting anisotropy, we respectively install perpendicular eddy current sensors on two measuring planes A and B.

Firstly, collecting a set of steady-state vibration data through the rotor test bench every 20 rpm within the range of speeds between 600 rpm and 3100 rpm, the sampling frequency is 2048 Hz, and the number of sampling points is 2048. After calculating the 126 sets of steady-state startup vibration data collected through Fast Fourier Transform, we will obtain the amplitude and phase values of rotating frequency component. Moreover, through verifying the amplitude and phase values of rotating frequency by spectral correction method, we will calculate more accurate amplitude and phase values of rotating frequency.

Then, collecting the continuous startup data through the rotor test bench every 20 rpm within the range of speeds between 600 rpm and 3100 rpm, and the sampling frequency is 2048 Hz, we will extract the rotating frequency component through parameterized time-frequency method. Moreover, according to its complex envelope,

we also obtain the amplitude and phase values of rotating frequency component.

Taking the root mean square error of formula (4) as evaluation index, the root mean square error of each channel is shown in Table 1.

Table 1. RMSE of rotating frequency components of continuous startup and steady-start startup

	$1-x$	$1-y$	$2-x$	$2-y$
Amplitude ( $\mu\text{m}$ )	1.3727	2.0116	1.1386	2.1934
Phase ( $^{\circ}$ )	0.1014	0.0984	0.1107	0.0916

The simulation signal analysis and steady-state startup experiment show that parameterized time-frequency analysis method can accurately extract the rotating frequency component during the rotor startup process, which possess excellent accuracy and reliability.

#### 4. Experiment of balancing

To conduct the balancing experiment on Bently RK4 rotor test bench, we have to set the sampling frequency to be 2048 Hz, and measure to obtain the startup vibration signal of the rotor system within the range of 600 rpm to 3100 rpm.

The rotating frequency component is extracted through using parameterized time-frequency method. Then, according to the complex envelope, we will obtain the amplitude and phase values of rotating frequency component.

Adding 0.6 g  $\angle 135^{\circ}$  trail weight to the rotor test bench A correction plane, 0.6 g  $\angle 225^{\circ}$  trial weight to the rotor test bench B correction plane, and maintaining the sampling parameters and speeding-up ratio unchanged, we once again measure the startup vibration signal on two planes A and B. We will extract the rotating frequency component through using parameterized time-frequency component, so as to obtain the amplitude and phase values of rotating frequency component.

According to the original startup vibration information and the trial weight added startup vibration information, we can obtain the transfer matrix of the rotor at every speed within the range of 600 rpm to 3100 rpm, that is, the transfer matrix of the rotor under all working conditions. Combined with holobalancing method, we can implement the balancing of rotor under all working conditions.

In order to verify the above balancing method under all working conditions, this thesis respectively chooses the vibration information at 1650 rpm and 2000 rpm to carry out balancing calculation. Moreover, it also chooses 3000 rpm as the working speed of the rotor to analyze its balance effect on the vibrations at the critical and working speed.

Firstly, choosing the vibration information at 1650 rpm to carry out holobalancing, and the weight meter calculation data is shown in Table 2.

Then, choosing the vibration information at 2000 rpm to carry out holobalancing, and the weight meter calculation data is shown in Table 3.

When choosing the vibration information at 1650 rpm to carry out holobalancing, the actual weight added to plane A is 0.9 g  $\angle 157.5^{\circ}$ , plane B is 1.1 g  $\angle 225^{\circ}$ . The

vibration amplitude values at the critical and working speeds before and after the balancing are shown in Table 4.

Table 2. The weight meter calculation table of 1650 rpm

Type	Plane A	Plane B
Original vibration ( $\text{m}(\circ)^{-1}$ )	49.37 $\angle$ 73.8	45.66 $\angle$ 83.4
Vibration of adding trial weight ( $\text{m}(\circ)^{-1}$ )	25.54 $\angle$ 95.3	24.58 $\angle$ 100.4
Balance weight ( $\text{g}(\circ)^{-1}$ )	0.87 $\angle$ 159.7	1.08 $\angle$ 230.3

Table 3. The weight meter calculation table of 2000 rpm

Type	Plane A	Plane B
Original vibration ( $\text{m}(\circ)^{-1}$ )	65.38 $\angle$ 247.78	59.6 $\angle$ 254.9
Vibration of adding trial weight ( $\text{m}(\circ)^{-1}$ )	25.93 $\angle$ 267.2	28.6 $\angle$ 279.4
Balance weight ( $\text{g}(\circ)^{-1}$ )	0.4 $\angle$ 125.4	1.28 $\angle$ 212.5

Table 4. The balancing effects of 1650 rpm

Speed	Position	Amplitude value before balancing (m)	Amplitude value after balancing (m)	Reduction ratio of amplitude value (%)
Critical speed	1 - $x$	264.694	33.4107	87.37
	1 - $y$	257.5569	44.5457	82.70
	2 - $x$	201.858	24.1402	88.04
	2 - $y$	258.068	44.4373	82.78
Working speed	1 - $x$	26.2071	13.6456	47.93
	1 - $y$	23.263	13.0152	44.05
	2 - $x$	22.9353	1.5554	93.21
	2 - $y$	26.6456	2.4085	90.96

When choosing the vibration information at 2000 rpm to carry out holobalancing, the actual weight added to plane A is 0.4 g  $\angle$  135°, plane B is 1.3 g  $\angle$  225°. The vibration amplitude values at the critical and working speeds before and after the balancing are shown in Table 5.

Figure 3 is the comparison of vibration amplitude value before and after balancing in four channels. According to the experimental results, it can be seen whether to use the vibration information of 1650 rpm or that of 2000 rpm, we can effectively reduce the vibration amplitude values at the critical and working speeds.



Table 5. The balancing effects of 2000 rpm

Speed	Position	Amplitude value before balancing (m)	Amplitude value after balancing (m)	Reduction ratio of amplitude value (%)
Critical speed	$1 - x$	264.694	20.317	92.32
	$1 - y$	257.5569	34.2177	86.71
	$2 - x$	201.858	12.7907	93.66
	$2 - y$	258.068	33.8346	86.89
Working speed	$1 - x$	26.2071	8.462	67.71
	$1 - y$	23.263	8.0702	65.31
	$2 - x$	22.9353	8.0465	64.92
	$2 - y$	26.6456	9.6458	63.80

## 5. Conclusion

This paper proposes a new method of controlling the vibration amplitude at the rotor system run-up stage under different speeds effectively, which can ensure the safety operation of rotor systems. In view of the shortage of the current rotor balancing method, this paper constructs appropriate rotation operator by the rotating frequency and rotates the time-frequency characteristics of the run-up signal based on parameterized time-frequency analysis theory, which can accurately extract the rotating frequency component. This balance method can effectively reduced the vibrations at the critical and working speeds, and we have carried out the experimental verification as well. Comparing the proposed and traditional balancing method, we have concluded the following three advantages:

(1) The acquisition of the signals is convenient, because we only need to collect the vibration data during the process of rotor startup, instead of the steady-state data at some certain speed.

(2) The number of startups is less. This method can obtain the transfer matrix of the rotor under full working conditions through only two times of rotor speeding-up startup processes, so as to achieve the balance of the rotor.

(3) The balance effect is excellent, which can effectively reduce the vibrations of the rotor at both working and critical speeds.

The proposed method in this paper can be used at the large-scale rotating machinery balance in practical industrial field. This method need the support of key-phase signal, which made this method may be restricted to use at some rotor without key-phase signal collection device.

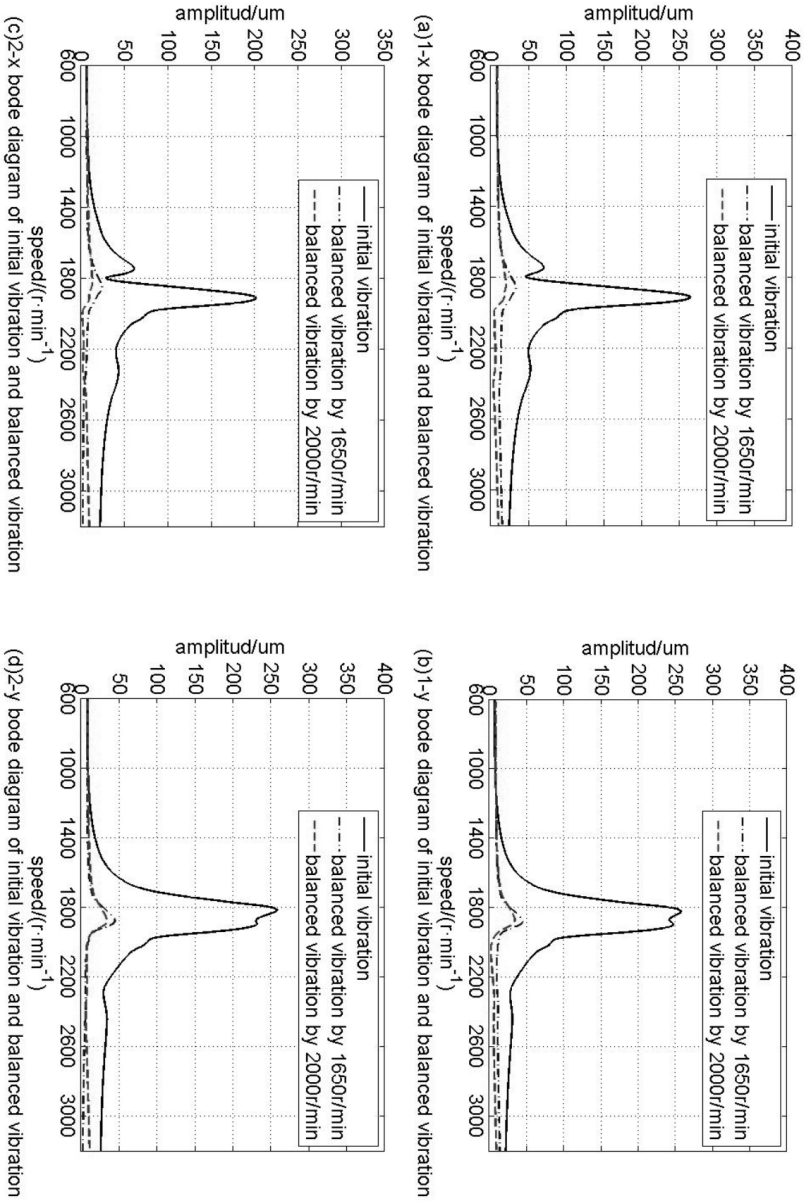


Fig. 3. The amplitude value Bode diagram of rotating frequency before and after balancing

**References**

- [1] S. LIU: *A modified low-speed balancing method for flexible rotors based on holospectrum*. Mechanical Systems and Signal Processing 21 (2007), No. 1, 348–364.
- [2] Y. KANG, T. W. LIN, Y. J. CHANG, Y. P. CHANG, C. C. WANG: *Optimal balancing of flexible rotors by minimizing the condition number of influence coefficients*. Mechanism and Machine Theory 43 (2008), No. 7, 891–908.
- [3] M. PALIWAL, U. A. KUMAR: *Neural networks and statistical techniques: A review of applications*. Expert Systems with Applications 36 (2009), No. 1, 2–17.
- [4] X. LI, L. ZHENG, Z. LIU: *Balancing of flexible rotors without trial weights based on finite element modal analysis*. Journal of Vibration and Control 19 (2013), No. 3, 461 to 470.
- [5] T. ARIMITSU: *Non-equilibrium thermo field dynamics and its application to error-correction for spatially correlated quantum errors*. Interdisciplinary Information Sciences 15 (2009), No. 3, 441–471.
- [6] Y. LEI, J. LIN, Z. HE: *A review on empirical mode decomposition in fault diagnosis of rotating machinery*. Mechanical Systems and Signal Processing 35 (2013), No. 1, 108–126.
- [7] S. GHOFRANI, D. C. MCLERNON: *Auto-Wigner-Ville distribution via non-adaptive and adaptive signal decomposition*. Signal Processing 89 (2009), No. 8, 1540–1549.
- [8] V. HUARD: *L'approche par compétences: Essais de modélisation dans le master « métiers de l'éducation et de la formation »*. Education Permanente (third term 2011), No. 188, 131–146.
- [9] D. JIANG, Z. XU, Z. CHEN, Y. HAN, H. XU: *Joint time–frequency sparse estimation of large-scale network traffic*. Computer Networks 55 (2011), No. 15, 3533–3547.
- [10] A. W. JASPER, S. J. KLIPPENSTEIN, L. B. HARDING, B. RUSCIC: *Kinetics of the reaction of methyl radical with hydroxyl radical and methanol decomposition*. Journal of Physical Chemistry A 111, (2007), No. 19, 3932–3950.
- [11] X. YANG, J. ZHU, L. QIU, D. LI: *Bioinspired effective prevention of restacking in multilayered graphene films: Towards the next generation of high-performance supercapacitors*. Advanced Materials 23 (2011), No. 25, 2833–2838.

Received July 12, 2017

